DOI: 10.1002/ange.201007262

# High-Temperature Wetting Transition on Micro- and Nanostructured Surfaces**

Tong Zhang, Jingming Wang,* Li Chen, Jin Zhai, Yanlin Song, and Lei Jiang*

With the discovery of novel wetting phenomena in nature, such as the self-cleaning effect of lotus leaves and the effortless stand and quick waterborne movement of water striders' legs, surfaces with special wettability have recently attracted significant attention and have become increasingly important in our daily lives.[1] Moreover, surface wettability at non-ambient temperature, especially at high temperature (above 100 °C), is of great importance in many industrial processes, including water transportation and metal processing, among others.[2] Recently, several advances have been made, such as the fabrication of thermally responsive materials with controllable wettability,[3] the repellent characteristics of different superhydrophobic surfaces to hot water,[4] application of hydrophobic surfaces on heat exchangers at low temperature,[5] evaporation-triggered wetting transition for water droplets on hydrophobic microstructures,[6] and enhancement of boiling by nanostructured interfaces.[7] The theory and applications of a liquid droplet bouncing on a hot surface in a solid–liquid heat transfer system, a very important phenomenon, have also been reported.[8] However, the effect of chemical composition and surface morphology on the wetting behavior at high temperature (above 100 °C) has not been studied systematically.

Herein, we report the investigation of the wetting behavior of surfaces with different chemical compositions and structures from 20 to 200 °C. Four kinds of micro- and nanostructured surfaces with different wettabilities were successfully fabricated. The wetting behavior of a water droplet was observed to be different on the surfaces, and the wetting transition (from spreading to bouncing) occurred at a specific temperature (i.e., the bouncing temperature, $T_b$) on hydrophilic, hydrophobic, and superhydrophilic surfaces. Surface wettability was crucial to the wetting-transition behavior, and surface roughness also affected the bouncing temperature of a surface ($T_b$). When surfaces with the same chemical composition got flatter, $T_b$ decreased at the superhydrophilic surfaces and hydrophobic surfaces, while it increased at the hydrophilic surfaces. However, the spreading–bouncing transition did not take place on superhydrophobic surfaces.

Silicon wafers with various structures were fabricated to investigate wettability at different temperatures. Wafers with micropillars and nanowire arrays (SiNWA) were obtained by lithography etching and chemical etching, respectively.[9] The samples were coated with fluoroalkylsilane (FAS) to obtain hydrophobic substrates.[10] Figure 1 shows the top-view scanning electron microscope (SEM) images and the static contact angle (CA) images of a water droplet before and after chemical modification with FAS at 25 °C. As shown in Figure 1 a, b, the unmodified flat silicon and microstructured silicon surfaces (MSis) exhibited hydrophilic characteristics, and the FAS-modified MSis (FAS-MSis) were hydrophobic. Correspondingly, in Figure 1 c, d, the unmodified nanostruc-

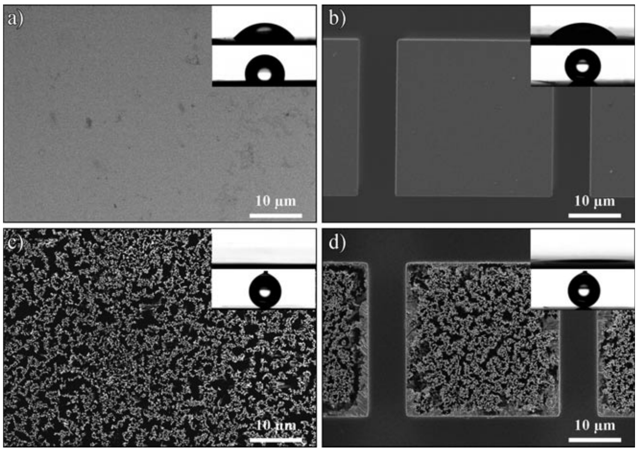

**Figure 1.** SEM images (top view) of silicon surfaces with hierarchical structure. The insets show the shape of water droplets on these surfaces before (top) and after FAS modification (bottom) at 25 °C. a) Flat silicon wafer. CA (54.2 ± 2.1)°/(106.4±0.5)° (before/after modification) b) Silicon wafer with micropillars. The side length $D$ of the micropillar is 30 μm, CA (41.1 ± 2.5)°/(144.8±0.4)°. c) Silicon wafer with nanowire arrays (SiNWA). CA 0°/(162.2±0.8)°. d) Silicon wafer with the composition of nanowire micropillars. $D = 30$ μm, CA 0°/(166.5±0.7)°.

---

[*] Dr. T. Zhang, Dr. L. Chen, Prof. Y. Song, Prof. L. Jiang
Beijing National Laboratory for Molecular Sciences (BNLMS)
Key Laboratory of Organic Solids
Institute of Chemistry, Chinese Academy of Sciences
Beijing 100190 (P. R. China)
Fax: (+86) 10-8262-7566
E-mail: jianglei@iccas.ac.cn
Dr. J. Wang, Prof. J. Zhai
School of Chemistry and Environment, Beihang University
Beijing 100191 (P. R. China)
E-mail: wangjm@buaa.edu.cn
Dr. T. Zhang, Dr. L. Chen
Graduate School of the Chinese Academy of Sciences
Beijing 100049 (P. R. China)

[**] We are grateful for financial support by the National Research Fund for Fundamental Key Projects (2010CB934700, 2009CB930404, 2007CB936403, 2009AA03Z339) and the National Natural Science Foundation (20920102036, 20974113). The Chinese Academy of Sciences is gratefully acknowledged. We also thank Zhongwei Sun, Mingjie Liu, and Hao Bai for technical support and helpful discussions.

Supporting information for this article is available on the WWW under http://dx.doi.org/10.1002/anie.201007262.

tured silicon and micro- and nanostructured silicon surfaces (MNSis) were superhydrophilic, with contact angles near 0°, while the FAS-modified MNSis (FAS-MNSis) were superhydrophobic ($CA > 160°$), such that the 2 μL water droplet could not descend but was stuck to the pinhead instead. The effect of the micropillar side length $D$ ($D = \infty$ represents surfaces without any microstructure) of the four different substrates on the water contact angle at 25 °C are shown in Figure S1 in the Supporting Information.

Subsequently, the wetting behavior of the four groups of surfaces (MSis, FAS-MSis, MNSis, and FAS-MNSis) at various temperatures was investigated. The schematic diagram of the experimental device is shown in Figure S5 in the Supporting Information. A heating stage with controllable temperature was used. The surface temperature and the water spreading or bouncing were recorded with a precise thermocouple and a CCD, respectively. The injector was kept 200 mm higher than the heating stage to preserve the drop from heat. Only when the stage temperature reached the test temperature was the injector rotated down, and a 3.5 μL water droplet was pushed out. After the water droplet left the needle of the injector, it was rotated again to the high position. The water droplet was well preserved before coming into contact with the high-temperature surfaces (see the Supporting Information for details).

Figure 2 shows the typical spreading and bouncing behavior of water droplets on surfaces with different wettabilities at temperatures above 100 °C. The droplet did not wet the surface but instead bounced on the surface at a certain temperature, which was called the bouncing temperature ($T_b$). For the hydrophilic smooth silicon surface (Figure 2a), the water droplet stood on the surface with a contact angle smaller than 60° before the surface temperature reached its $T_b$ at 183 °C and then evaporated quickly. When the surface was heated to 183 °C or above, the water droplet wetted the surface and then bounced up with a contact time of about 0.16 s. Similarly, $T_b$ of the hydrophobic surface was 164 °C. The droplet stood on the hydrophobic smooth silicon surface modified with FAS with a contact angle larger than 100° and evaporated slowly when the surface temperature was lower than its $T_b$ at 164 °C (Figure 2b), but bounced up slightly with a longer contact time of about 0.4 s when the temperature reached or exceeded 164 °C. In comparison, the droplet evaporated and disappeared immediately when the temperature of the superhydrophilic surface was lower than its $T_b$ at 152 °C (Figure 2c). In cases when the surface temperature was higher than 152 °C, the droplet on the superhydrophilic surface bounced so strongly and quickly that the contact time between the droplet and the surface was less than 0.04 s. No bouncing occurred on the FAS-modified superhydrophobic surface with SiNWA (Figure 2d). At lower temperatures (e.g., 60 °C), the droplet pinned on the surface and evaporated very slowly, but at higher temperature (80 °C), below the boiling point of water, the droplet rolled away after being dropped on the surface.

At a given temperature, the vaporizing velocity of a droplet clearly depends on the heat-transfer ability of the surface. The more heat is transferred through the solid–liquid interface, the faster the droplet vaporizes. Hence, the wetting and bouncing processes both indicated that the superhydrophilic surface had excellent heat-transfer ability. The drop evaporated very fast below $T_b$, and above $T_b$, the bottom part of the droplet evaporated faster and formed a vapor film to bounce the droplet up in less than 0.04 s, which was much faster than on the hydrophilic and hydrophobic surfaces. In comparison, the droplet stood on the superhydrophobic surface with a contact angle larger than 150° and evaporated very slowly at lower temperature and did not wet but rolled away at 80 °C. The small velocity of vaporization demonstrated the poor heat-transfer ability of the superhydrophobic surface.

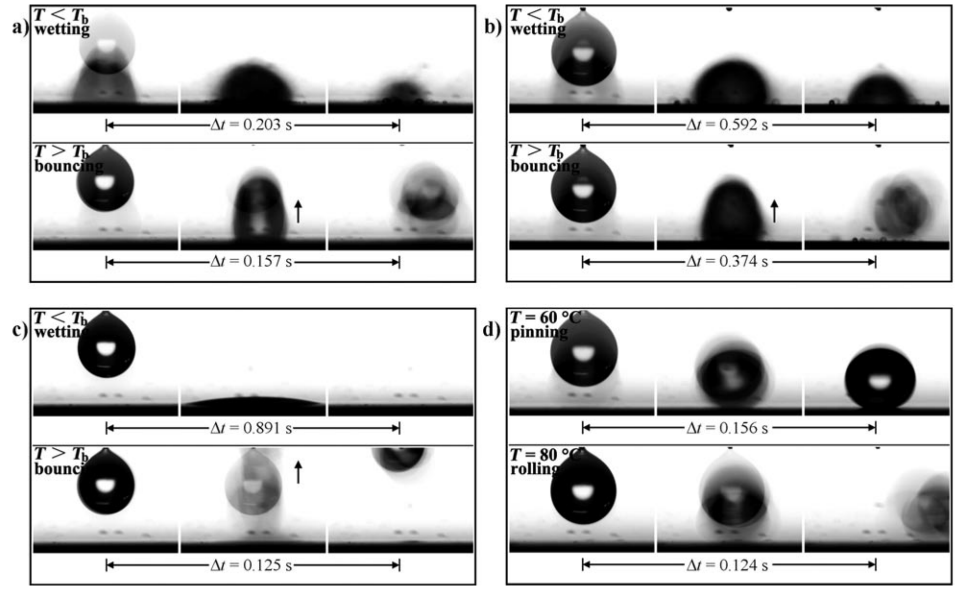

***Figure 2.*** Video snapshots of typical wetting and bouncing behavior of water droplets on high-temperature surfaces. a) Unmodified flat hydrophilic silicon surface, $T_b = 183$ °C. b) FAS-modified flat hydrophobic silicon surface, $T_b = 164$ °C. c) Unmodified superhydrophilic SiNWA, $T_b = 152$ °C. d) FAS-modified superhydrophobic SiNWA surface. No bouncing occurred on this surface.

Although substrates with similar structures, such as the MSis, exhibited similar high-temperature spreading and bouncing and had similar contact times in the bouncing process, $T_b$ of surfaces with similar contact angles varied with the change of surface roughness. Figure 3 shows the relationship between surface roughness and $T_b$ for MSis, MNSis, and FAS-MSis. With an increase in $D$ (from 10 μm to infinity), $T_b$ increased for the hydrophilic MSis (from 157 to 183 °C) while it decreased for the hydrophobic FAS-MSis (from 186 to 164 °C)

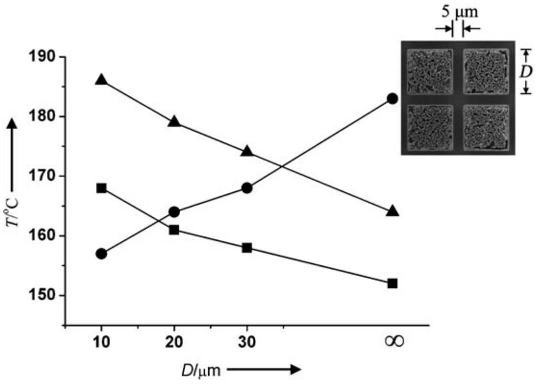

*Figure 3.* The bouncing temperature ($T_b$) with different micropillar side lengths $D$. $D=\infty$ represents the surfaces without any microstructure. ●: Microstructured hydrophilic surfaces (MSis). ▲: Microstructured hydrophobic surfaces (FAS-MSis). ■: Micro- and nanostructured superhydrophilic surfaces (MNSis).

and superhydrophilic MNSis (from 168 to 152 °C). $T_b$ of the hydrophilic MSis was higher than the superhydrophilic MNSis for $D \geq 20$ μm.

The comparisons between the $T_b$ of different surfaces remind us that, although the superhydrophilic MNSis could enhance heat transfer between solid and water, the droplet would bounce on them at a lower temperature compared with the hydrophilic MSis. Furthermore, if the surface temperature is above $T_b$, a vapor film would be generated. Therefore, for equipment with strict and high working temperature, the surface with a higher $T_b$ should be chosen.

Two theoretical models of the wetting state at high temperature have been proposed to explain the change in $T_b$ (Figure 4). It is understood that a set volume of vapor film has to be produced by phase transition to bounce a given droplet. Throughout the bouncing process, the internal temperature of the water droplets changed little. Therefore, the vaporization velocity and the vapor film formation could only be influenced by the change of surface conditions (Supporting Information S6).[11] As shown in Figure 4, the volume of vapor film can be expressed as in Equation (1):

$$V = A(v_v - v_w)t \qquad (1)$$

where $V$ is the volume of vapor film, $A$ is the wetting area between solid and liquid, $v_v$ is the vaporizing velocity that changes with surface temperature, $v_w$ is the rewetting velocity controlled by the contacting solid and liquid, and $t$ is the time of wetting before bouncing. When the droplet made contact with the unmodified MSis and the MNSis with high surface energy, it was in a Wenzel state, in which the liquid completely fills the grooves of the rough surface.[12] According to Figure 4a and Equation (1), if $V$ and $v_w$ are invariable and $t$ changes little on similar surfaces, then $v_v$ must decrease with the increase in $A$, and $T_b$ would decrease as well. For the hydrophilic MSis, the wetting area between silicon and water decreases when $D$ increases (see the Supporting Information). Hence, $T_b$ exhibits the same change as $D$. For the MNSis, $A$ decreases with a decrease in $D$, so $T_b$ decreased when $D$ increased. Furthermore, nanostructured surfaces have far larger specific surface areas than microstructured surfaces, so the value of $A$ for MNSis is much larger than that of MSis, which makes $t$ for MNSis much shorter than the other bounced series of surfaces. In contrast, FAS-MSis and FAS-MNSis exhibited the Cassie state when drops made contact with them. In the Cassie state, $A$ becomes larger as the surface gets flatter, because air remains in the micro- and nanogrooves. For FAS-MSis, the longer $D$ is, the larger $A$ becomes, and $T_b$ decreases accordingly. However, according to the Cassie equation, if a surface exhibits excellent superhydrophobic characteristics with a contact angle near 180°, the droplet cannot wet the surface but would be separated from the solid by an almost continuous air film. The Cassie equation is defined as in Equation (2):

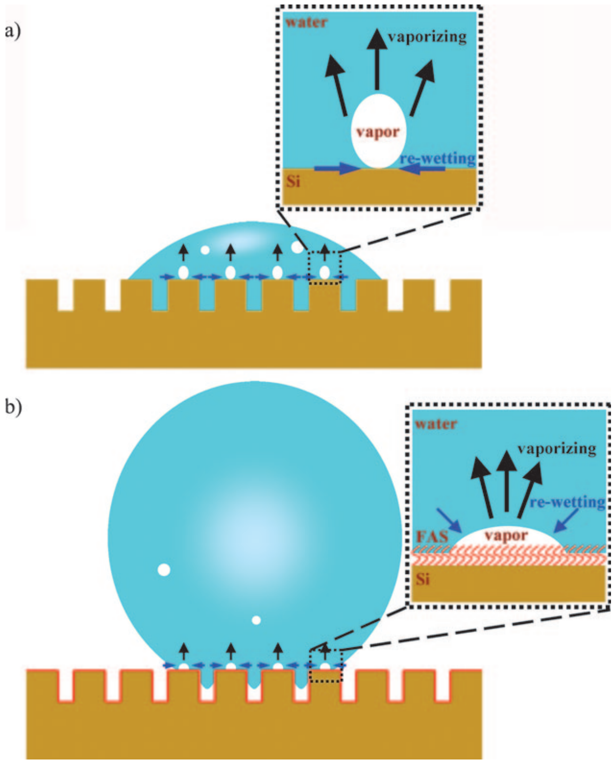

*Figure 4.* Two proposed mechanisms of the wetting state at high temperature. a) Wetting details of the Wenzel state at high temperature. Air bubbles are generated quickly and escape from the hydrophilic surface easily. b) Wetting details of the Cassie state at high temperature. Air bubbles are generated slowly and prefer to stick on the hydrophobic surface for a longer time.

$$\cos\theta_C = f_s(\cos\theta + 1) - 1 \qquad (2)$$

where $f_s$ is the area fraction of the solid.[13] If $\theta_C$ is close to 180°, then $f_s$ would be quite tiny as it approaches 0. As a result, $v_v$ would be near 0, too. Thus, the droplet could not bounce on the superhydrophobic FAS-MNSis but rolled away with a slight imbalance. More evidence can be seen in Supporting Information.

In summary, the typical wetting transition on micro- and nanostructured surfaces with different wettabilities at high temperature has been investigated. Experimental results indicate that both surface wettability and surface roughness are crucial to the wetting transition behavior. The spreading–bouncing transition occurred on hydrophilic, hydrophobic, and superhydrophilic surfaces above 100 °C. When the side length of micropillars on substrates increased from 10 μm to infinity (i.e., no micropillars), $T_b$ decreased for the superhydrophilic MNSis and hydrophobic FAS-MSis, while it increased for the hydrophilic MSis. However, the spreading–bouncing transition could not take place on superhydrophobic FAS-MNSis. The two proposed mechanisms of wetting at high temperature explained the transition phenomena well. Moreover, the high-temperature wetting transition could be potentially valuable in water transportation and other industrial applications, such as material choice in liquid–solid systems working at non-ambient temperature.

## Experimental Section

Instruments and characterization: SEM images of the samples were obtained using a field-emission scanning electron microscope (JSM-6700F, Japan). Contact angles were measured on an OCA20 instrument (DataPhysics, Germany) at 25 °C. Deionized water droplets (about 2 μL) were dropped carefully onto the surface. The average contact angle value was obtained by measuring at five different positions of the same sample.

Fabrication of SiNWA: Cut silicon wafers were soaked in $H_2SO_4$/$H_2O_2$ ($H_2SO_4$ (97 %)/$H_2O_2$ (30 %) = 3:1) for 30 min at 80 °C, then rinsed with deionized water four or five times. Cleaned silicon strips were put into the etching solution (HF 5.0 mol$L^{-1}$ and $AgNO_3$ 0.015 mol$L^{-1}$), sealed at 50 °C for 25 min, then immersed in 20 % nitric acid for 30 s and finally rinsed with deionized water four or five times.

Modification with FAS: Cleaned silicon strips with microstructures were put into a sealed container together with a piece of glass coated with about 0.5 mL FAS. Then the container was then evacuated with a vacuum pump, and the vacuum was maintained vacuum for 12 h.

Received: November 18, 2010
Revised: February 21, 2011

**Keywords:** high-temperature chemistry · hydrophobic effect · microstructure · surface chemistry · wettability

[1] a) M. J. Liu, Y. M. Zheng, J. Zhai, L. Jiang, *Acc. Chem. Res.* **2010**, *43*, 368 – 377; b) T. L. Sun, L. Feng, X. F. Gao, L. Jiang, *Acc. Chem. Res.* **2005**, *38*, 644 – 652; c) L. Feng, S. H. Li, Y. S. Li, H. J. Li, L. J. Zhang, J. Zhai, Y. L. Song, B. Q. Liu, L. Jiang, D. B. Zhu, *Adv. Mater.* **2002**, *14*, 1857 – 1860; d) X. J. Feng, L. Jiang, *Adv. Mater.* **2006**, *18*, 3063 – 3078; e) F. Xia, L. Jiang, *Adv. Mater.* **2008**, *20*, 2842 – 2858; f) J. K. Yuan, X. G. Liu, O. Akbulut, J. Q. Hu, S. L. Suib, J. Kong, F. Stellacci, *Nat. Nanotechnol.* **2008**, *3*, 332 – 336; g) D. Quere, M. Reyssat, *Philos. Trans. R. Soc. London Ser. A* **2008**, *366*, 1539 – 1556; h) J. B. Boreyko, C. H. Chen, *Phys. Rev. Lett.* **2009**, *103*, 184051.

[2] a) J. Hashim, L. Looney, M. S. J. Hashmi, *J. Mater. Process. Technol.* **2001**, *119*, 324 – 328; b) J. Hashim, L. Looney, M. S. J. Hashmi, *J. Mater. Process. Technol.* **2001**, *119*, 329 – 335.

[3] a) T. L. Sun, G. J. Wang, L. Feng, B. Q. Liu, Y. M. Ma, L. Jiang, D. B. Zhu, *Angew. Chem.* **2004**, *116*, 361 – 364; *Angew. Chem. Int. Ed.* **2004**, *43*, 357 – 360; b) N. Wang, Y. Zhao, L. Jiang, *Macromol. Rapid Commun.* **2008**, *29*, 485 – 489.

[4] Y. Liu, X. Chen, J. Xin, *J. Mater. Chem.* **2009**, *19*, 5602 – 5611.

[5] S. Daniel, M. K. Chaudhury, J. C. Chen, *Science* **2001**, *291*, 633 – 636.

[6] P. C. Tsai, R. G. H. Lammertink, M. Wessling, D. Lohse, *Phys. Rev. Lett.* **2010**, *104*, 116102.

[7] a) S. H. Li, R. Furberg, M. S. Toprak, B. Palm, M. Muhammed, *Adv. Funct. Mater.* **2008**, *18*, 2215 – 2220; b) R. Chen, M. C. Lu, V. Srinivasan, Z. Wang, H. H. Cho, A. Majumdar, *Nano Lett.* **2009**, *9*, 548 – 553; c) C. Li, Z. Wang, P. I. Wang, Y. Peles, N. Koratkar, G. P. Peterson, *Small* **2008**, *4*, 1084 – 1088.

[8] a) M. Elbahri, D. Paretkar, K. Hirmas, S. Jebril, R. Adelung, *Adv. Mater.* **2007**, *19*, 1262 – 1266; b) C. T. Avedisian, J. Koplik, *Int. J. Heat Mass Transfer* **1987**, *30*, 379 – 393; c) J. Bernardin, I. Mudawar, *J. Heat Transfer* **1999**, *121*, 894; d) H. Linke, B. J. Aleman, L. D. Melling, M. J. Taormina, M. J. Francis, C. C. Dow-Hygelund, V. Narayanan, R. P. Taylor, A. Stout, *Phys. Rev. Lett.* **2006**, *96*, 154502; e) A. L. Biance, C. Clanet, D. Quere, *Phys. Fluids* **2003**, *15*, 1632 – 1637.

[9] K. Peng, Y. Yan, S. Gao, J. Zhu, *Adv. Funct. Mater.* **2003**, *13*, 127 – 132.

[10] A. Nakajima, A. Fujishima, K. Hashimoto, T. Watanabe, *Adv. Mater.* **1999**, *11*, 1365 – 1368.

[11] a) T. Kudra, Y. Pan, A. Mujumdar, *Drying Technol.* **1991**, *9*, 693 – 707; b) Y. Ge, L. S. Fan, *Int. J. Heat Mass Transfer* **2006**, *49*, 4231 – 4249; c) N. Nikolopoulos, A. Theodorakakos, G. Bergeles, *Int. J. Heat Mass Transfer* **2007**, *50*, 303 – 319.

[12] R. Wenzel, *Ind. Eng. Chem.* **1936**, *28*, 988 – 994.

[13] A. Cassie, S. Baxter, *Trans. Faraday Soc.* **1944**, *40*, 546 – 551.